

# Densified multiwalled carbon nanotubes–titanium nitride composites with enhanced thermal properties

Linquin Jiang, Lian Gao<sup>1,\*</sup>

*State Key Laboratory of High Performance Ceramics and Superfine Microstructure, Shanghai Institute of Ceramics,  
Chinese Academy of Sciences, Shanghai 200050, PR China*

Received 3 February 2006; received in revised form 27 July 2006; accepted 10 September 2006

Available online 7 November 2006

## Abstract

Densified multiwalled carbon nanotube (MWNT)–TiN composites with various MWNTs contents were successfully obtained through a spark plasma sintering (SPS) method. The thermal conductivity  $k$  was found to increase with the MWNT amount and temperature. In the presence of 5 wt% MWNTs, there was a 97% enhancement in  $k$  at 703 K compared with that of TiN. The high thermal conductivity of MWNTs, a good interfacial combination and a homogeneous dispersion of MWNTs are key issues to enhance the thermal conductivity of MWNT–TiN composites. © 2006 Elsevier Ltd and Techna Group S.r.l. All rights reserved.

**Keywords:** B. Composites; C. Thermal properties; D. Nitrides; Carbon nanotubes

## 1. Introduction

Carbon nanotubes (CNTs) are proposed as fillers in CNTs composites based on their unique physical properties [1–4]. In particular, a recent value of  $3000 \text{ W m}^{-1} \text{ K}^{-1}$  for the thermal conductivity of an individual MWNT [5], which is remarkably higher than for any known thermal conducting materials of diamond or graphite, shows that superior thermal properties of the graphite plane are realized by carbon nanotubes. Extremely high thermal conductivity is theoretically predicted for CNT, due to large phonon mean free path in strong carbon  $\text{sp}^2$  bond network of CNT walls [6,7]. Many efforts have been focused on the increase in the thermal conductivity of organic fluids or polymers filled with relatively low concentration of CNTs [8,9]. The obtained results are intriguing for the researchers. For example, Biercuk et al. [6] fabricated SWNT-epoxy composites and measured a thermal conductivity enhancement greater than 125% at 1.0 wt% nanotube loading. Liu et al. [10] found the thermal conductivity to exhibit a 65% enhancement with 3.8 wt% CNT loading in CNT-silicone elastomer composite. In addition, thermal conductivity enhancement has been observed in CNT suspensions [9,11,12].

However, there is few study on the thermal properties of CNT-ceramic composites [13]. The investigations on inorganic solid composites containing CNTs are quite difficult, since homogeneous dispersion of the CNTs is more difficult to achieve in solid composites than in liquid [10,13]. Especially there are few reports on the thermal conductivities of dense nitride-CNTs composites until now. Titanium nitride (TiN) is a very important material widely used as coating material and in semiconductor industry for its high hardness, abrasion resistance, as well as excellent electrical and thermal transfer properties [14,15]. In this paper, dense MWNTs–TiN composites with various MWNTs contents were successfully fabricated by SPS technology. The microstructure and the thermal properties including thermal capacity, thermal diffusivity and thermal conductivity, were systematically investigated.

## 2. Experimental procedure

MWNTs with diameters of 10–30 nm and lengths of 2–500  $\mu\text{m}$  (Shenzhen Nanotech Port Co. Ltd.) were oxidized by refluxing at  $140^\circ\text{C}$  in concentrated nitric acid for 6 h. The obtained acidic MWNTs were dispersed in distilled water by ultrasonication. 10 vol% of  $\text{Ti}(\text{OC}_4\text{H}_9)_4$ /ethanol solution was dripped into the above stirred MWNTs suspension until the final  $\text{Ti}:\text{H}_2\text{O}$  molar ratio reached 1:150. After further rinsing

\* Corresponding author. Tel.: +86 21 52412718; fax: +86 21 52413122.

E-mail address: [liangao@online.sh.cn](mailto:liangao@online.sh.cn) (L. Gao).

<sup>1</sup> Member, American Ceramic Society.

and drying, the Ti precursor with MWNTs was calcinated at 300 °C for 2 h. Then the composite powder was loaded into a quartz boat and heated in flowing  $\text{NH}_3$  ( $1 \text{ L min}^{-1}$ ) at 800 °C for 5 h in a tube furnace to obtain MWNTs–TiN composite. According to the initial additive content of the acidic MWNTs (in wt%: 0, 0.1, 1 and 5), the obtained composites are designated as TN, TNC-0.1, TNC-1 and TNC-5, respectively, as seen in Table 1.

Using as-prepared composite powders, disks of 10 mm in diameter and 2 mm in thickness were obtained by SPS (Dr. Sinter 2080 SPS apparatus) at 1250 °C under 50 MPa for 2 min in vacuum. The composition of the composites was characterized by X-ray powder diffraction (XRD, D/max 2550 V, Rigaku, Japan). Raman spectra (Labram-1B, JY Co., France) of MWNTs and MWNTs–TiN composites were recorded at room temperature, using a Micro-Raman system. Transmission electron microscopy (TEM, JEM 2100F, JEOL, Tokyo, Japan), energy-dispersive spectroscopy (EDS, Model ISIS, Oxford Microanalysis Group, Link, High Wycombe, UK) and field emission scanning electron microscopy (SEM, JSM 6700F, JEOL, Tokyo, Japan) were used to observe the fracture surfaces of the MWNT–TiN composites. Archimedes' method was used to measure the composite density. The density of pure TiN and MWNTs is 5.4 and  $2.1 \text{ g cm}^{-3}$  (claimed by the manufacturer), respectively. Specific heat capacity values were obtained by using a thermal analysis meter (DSC-2C, USA). The laser flash method was adopted to measure the thermal diffusivity using the Netzsch LFA427 measuring apparatus (Netzsch, Bayern, Germany).

### 3. Results and discussion

XRD patterns of the MWNT–TiN composites obtained after nitridation are shown in Fig. 1. The XRD peaks correspond well with the reported values of TiN (JCPDS 87-0682). Due to the restriction of XRD measurement, the content of MWNTs below 5 wt% in the composite is not well detected. For clarification, the small peak at  $26.06^\circ$  for TNC-5 composite, which is attributed to the characteristic peak of MWNTs, is enlarged by five times. The existence of the characteristic peak indicates the preservation of MWNTs in the composite after SPS sintering.

Raman spectroscopy was used to further investigate the characteristic structures and properties of MWNTs after SPS sintering. Raman spectra of pure MWNTs and MWNTs–TiN composites with various MWNTs contents are shown in Fig. 2. In the frequency range from 1200 to  $1700 \text{ cm}^{-1}$ , two peaks were observed at 1323 and  $1578 \text{ cm}^{-1}$ . The peak at  $1323 \text{ cm}^{-1}$

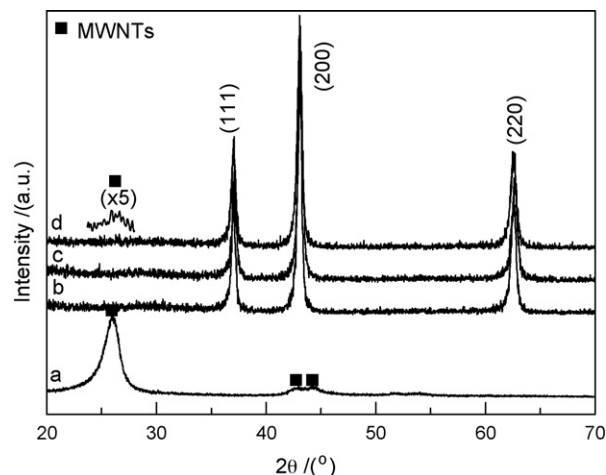


Fig. 1. XRD patterns of (a) MWNTs, (b) TNC-0.1, (c) TNC-1 and (d) TNC-5 composites. To clarify the peak of MWNTs, the XRD peak is magnified by five times ( $5\times$ ).

corresponds to disorder-induced phonon mode (D-band) of MWNTs, and the peak at  $1578 \text{ cm}^{-1}$  can be assigned to  $\text{E}_{2\text{g}}$ -band of MWNTs. The incorporation of MWNTs in the composite after SPS sintering does not produce a significant change in the Raman peak location of the nanotube breathing modes, indicating that the tubular structure of the nanotube is essentially preserved [16,17]. The intensity of the band located at  $1323 \text{ cm}^{-1}$  increases with increasing feeding mass ratio of MWNT to TiN, implying the increase of MWNT content of the composites [18]. There is a lot of experimental evidence that any sidewall derivatisation of carbon nanotubes significantly changes the ratio of D/G line intensities [19,20]. From Fig. 2, the D/G line ratio of MWNTs changes after incorporation with TiN matrix, which is supposed due to the interfacial interaction between MWNTs and TiN. In our previous work, the chemical adsorption between MWNTs and TiN was confirmed [21]. Raman results indicate that MWNTs in the composites maintain their characteristic structures, which consist with the SEM observations (see the discussion below), and have interacted with TiN.

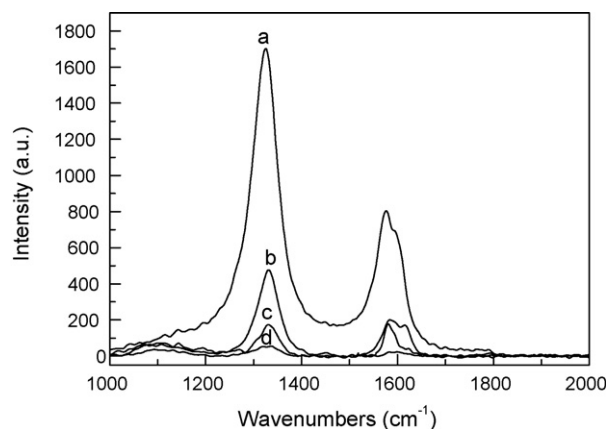


Fig. 2. Raman spectra of (a) MWNTs, (b) TNC-5, (c) TNC-1 and (d) TNC-0.1 composites.

Table 1  
Properties of MWNT-reinforced TiN nanocomposites consolidated by spark-plasma sintering at 1250 °C for 2 min

Materials	MWNTs content (wt%)	MWNTs content (vol%)	Relative density (% TD)
TN	0	0	100
TNC-0.1	0.1	0.26	100
TNC-1	1	2.55	98.6
TNC-5	5	12.0	97.8

The microstructure of the MWNT–TiN composite powders is shown in Fig. 3a. The EDS spectrum (inset in Fig. 3a) indicates that nanoparticles anchored on the nanotubes consist of TiN. The tiny TiN nanoparticle is well attached onto the outwall of the MWNTs, with a diameter of ca. 5–10 nm. SEM images of pure TiN and dense MWNT–TiN composites in the presence of 0.1, 1 and 5 wt% MWNTs are also shown in Fig. 3b–e. The nanotubes clearly survived from the processing and sintering, which is consistent with the XRD and Raman results. For the pure TiN ceramic, the size of a single hexagonal TiN grain is 100–150 nm. The morphology of the cross section has clear edges and corners, which denotes the intergranular

fracture mode. With the addition of MWNTs, the interface of grains becomes blurry and rugged, suggesting both the intergranular and the intragranular fracture modes exist in the composites. No notable agglomerates or phase separation between carbon nanotubes and TiN matrix are observed and MWNTs appear as individual with random orientation. Uniform dispersion and the interfacial conjunction of MWNTs in the matrix are important issues that affect the properties of the composites [10]. Based on the homogeneous distribution of MWNTs in the matrix and good interfacial interaction, severe aggregation of MWNTs was not found in SEM images with increasing MWNT content. However, the relative density of the composites decreases with increasing MWNT content, as seen in Table 1. The main reason is that more quantity of MWNTs in the matrix leads to more interfaces and pores, and inevitably some MWNTs aggregation appear, which decrease the relative density of MWNTs–TiN composites.

Thermal properties including specific heat capacity ( $C_p$ ), thermal diffusivity ( $\alpha^2$ ) and thermal conductivity ( $k$ ) of MWNTs–TiN composites have been investigated in detail. The  $C_p$ ,  $\alpha^2$  and  $k$  of both pure TiN and MWNT–TiN composites with various MWNTs contents versus temperature are shown in Fig. 4. In the measured temperature region, the  $C_p$  values slightly increase with increasing temperature. The  $C_p$  values are also found to increase with the MWNT amount. It has been reported that the increase of  $C_p$  in these composites is due to the contribution of MWNTs [13]. In the presence of 0.1 wt% MWNTs, the value of  $C_p$  is similar to that of pure TiN.

The thermal diffusivity ( $\alpha^2$ ) is a measure of the phonon mean free path. It is more recently appreciated that phonons dominate thermal transport at all temperatures in carbon materials [8,22]. In general, the values of  $\alpha^2$  increase with the temperature in the measured region as shown in Fig. 4b. An interesting phenomenon must be noted, that is, the  $\alpha^2$  shows abnormal high value in the presence of 0.1 wt% (0.26 vol%) MWNTs. Due to the high aspect ratio, the percolation threshold for nanotube composites can be well below 1% in volume [8,23]. The conducting nanotubes distribute randomly in the matrix connect the opposite faces of the matrix to act as passages for transporting thermal energy [25]. This, in principle, should allow for rapid heat flow along the percolated tube network and further enhancement of thermal transport [23]. The thermal diffusivities of the composites decrease upon further nanotube addition ( $f > 1$  vol%). The reduced thermal diffusivity indicates enhanced phonon scattering, possibly due to covalent interaction between MWNTs and TiN. Such interaction will act as scattering centers for phonons propagating along the tube axis, thus reducing thermal diffusivity of the composites [24]. Moreover, with further nanotube addition, the turbostratic stacking of adjacent walls is more significant to reduce the mean free path [25,26].

Thermal conductivities ( $k$ ) of the MWNT–TiN composites are calculated following the equation  $k \approx \alpha^2 C_p \rho$ . Here  $\rho$  is the density of the composites and measured by Archimede's method. With the increase of the temperature and MWNT amounts, the thermal conductivities of MWNT–TiN composites increase. It has been suggested that a covalent attachment between the

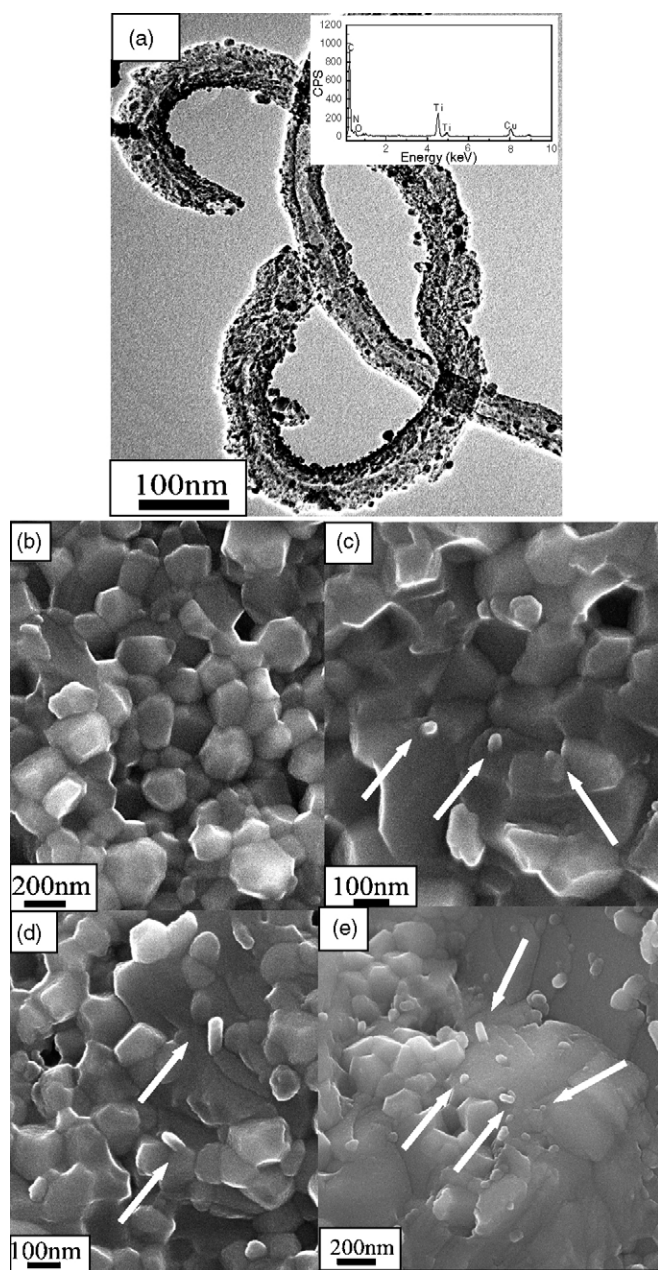


Fig. 3. (a) A typical TEM image and EDS spectrum of MWNT–TiN powder; and SEM images of (b) pure TiN ceramic and MWNT–TiN densified composites in the presence of (c) 0.1 wt%, (d) 1 wt%, and (e) 5 wt% MWNTs, respectively.



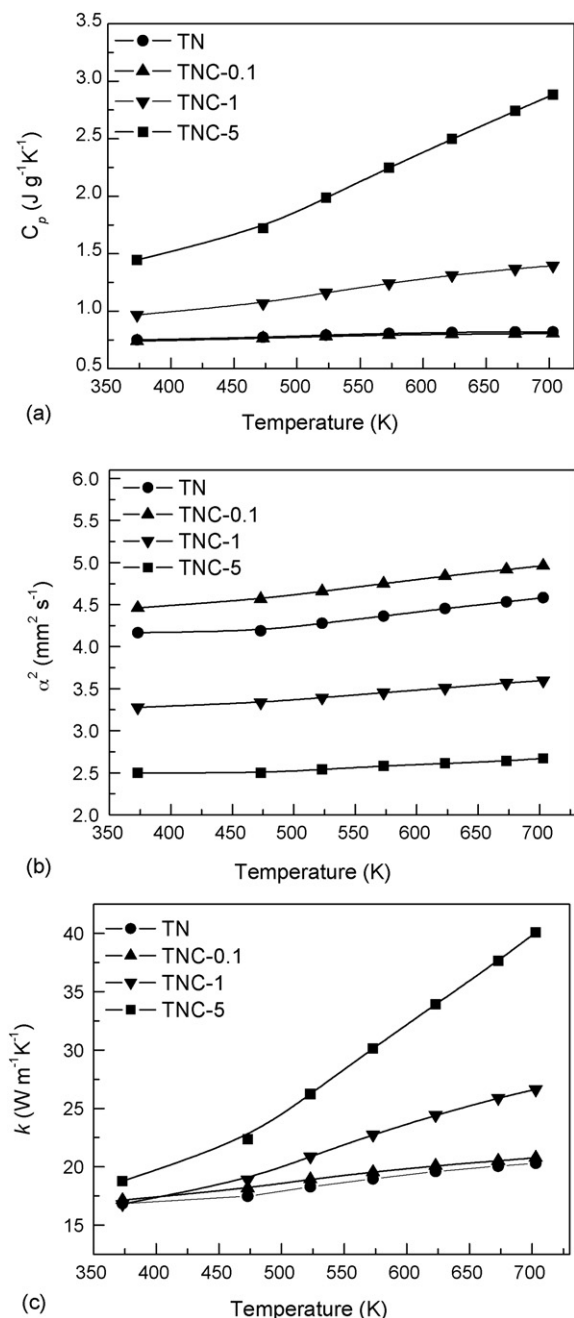


Fig. 4. Temperature dependence of (a) specific heat capacity, (b) thermal diffusivity, and (c) thermal conductivity of MWNT–TiN composites with various MWNT contents.

nanotube and the matrix is an effective way to alleviate negative effects of large interfacial resistance present in carbon nanotube composites [23]. To synthesize the MWNT–TiN composites, the functionalized nanotube with acidic groups was used to realize the covalent attachment of TiN nanoparticles to the tubes [21]. The thermal conductivity  $k$  was found to increase with both increasing MWNT amounts and temperature. In Fig. 4c, in the presence of 5 wt% MWNTs, the thermal conductivity of the composite exhibits an enhancement of 11% compared to that of pure TiN ceramic at 373 K. At 703 K, there is a 97% enhancement in  $k$  with 5 wt% MWNTs loading.

How the MWNTs enhance the thermal conductivity of the composite may be attributed to the reasons below. First, it is well known that the thermal conductivity of MWNTs ( $3000 \text{ W m}^{-1} \text{K}^{-1}$ ) is several orders of magnitude higher than that of pure TiN ceramics ( $16.8 \text{ W m}^{-1} \text{K}^{-1}$ ). The ultrahigh thermal conductivity of the nanotubes incorporated with the TiN matrix enhances the thermal conductivity of the composites [27]. Second, covalent combination of MWNTs and TiN [21] are beneficial to reduce tube-matrix thermal boundary resistance and thus improve the thermal conductivity of the composites. From SEM images, no phase separation between the carbon nanotubes and TiN matrix, and a great aggregation of the nanotubes in the matrix are observed, which indicate an effective interfacial interaction is realized. Third, a good dispersion of MWNTs in the TiN matrix observed from SEM images facilitates a sufficient loading of MWNTs with ultrahigh thermal conductivity to the matrix.

#### 4. Conclusions

This work reports the fabrication of dense MWNT–TiN composites by SPS in the presence of various MWNT amounts with enhanced thermal conductivities. Raman results and microstructure investigation indicate that MWNTs in the composites maintain their characteristic structures and a good interfacial interaction between the nanotubes and TiN are obtained. The thermal conductivity  $k$  was found to increase with increasing MWNT amounts and temperature. In the presence of 5 wt% MWNTs, there was a 97 and 11% enhancement in  $k$  at 703 and 373 K, respectively, compared with that of TiN. The ultrahigh thermal conductivity of the nanotubes in the matrix, a tight interfacial interaction and a homogeneous distribution of MWNTs enhance the thermal conductivity of the composites.

#### Acknowledgment

Authors thank for the support from National Natural Science Foundation of China (Nos. 50372077 and 50572114).

#### References

- [1] X.J. Xu, M.M. Thwe, Mechanical properties and interfacial characteristics of carbon-nanotube-reinforced epoxy thin films, *Appl. Phys. Lett.* 81 (15) (2002) 2833–2835.
- [2] F.T. Fisher, R.D. Bradshaw, L.C. Brinson, Effects of nanotube waviness on the modulus of nanotube-reinforced polymers, *Appl. Phys. Lett.* 80 (24) (2002) 4647–4649.
- [3] D. Qian, E.C. Dickey, R. Andrews, T. Rantell, Load transfer and deformation mechanisms in carbon nanotube-polystyrene composites, *Appl. Phys. Lett.* 76 (20) (2000) 2868–2870.
- [4] C. Bower, R. Rosen, L. Jin, J. Han, O. Zhou, Deformation of carbon nanotubes in nanotube-polymer composites, *Appl. Phys. Lett.* 74 (22) (1999) 3317–3319.
- [5] P. Kim, L. Shi, A. Majumdar, P.L. McEuen, Thermal transport measurements of individual multiwalled nanotubes, *Phys. Rev. Lett.* 87 (21) (2001) 215502–215505.
- [6] S. Berber, Y.-K. Kwon, D. Tomanek, Unusually high thermal conductivity of carbon nanotubes, *Phys. Rev. Lett.* 84 (20) (2000) 4613–4616.

- [7] D.J. Yang, Q. Zhang, G. Chen, S.F. Yoon, J. Ahn, S.G. Wang, Q. Zhou, Q. Wang, J.Q. Li, Thermal conductivity of multiwalled carbon nanotubes, *Phys. Rev. B* 66 (2002) 165440–165445.
- [8] M.J. Biercuk, M.C. Llaguno, M. Radosavljevic, J.K. Hyun, A.T. Johnson, Carbon nanotube composites for thermal management, *Appl. Phys. Lett.* 80 (15) (2002) 2767–2769.
- [9] S.U.S. Choi, Z.G. Zhang, W. Yu, E.A. Lockwood, E.A. Grulke, Anomalous thermal conductivity enhancement in nanotube suspensions, *Appl. Phys. Lett.* 79 (14) (2001) 2252–2254.
- [10] C.H. Liu, H. Huang, Y. Wu, S.S. Fan, Thermal conductivity improvement of silicone elastomer with carbon nanotube loading, *Appl. Phys. Lett.* 84 (21) (2004) 4248–4250.
- [11] H. Xie, H. Lee, W. Youn, M. Choib, Nanofluids containing multiwalled carbon nanotubes and their enhanced thermal conductivities, *J. Appl. Phys.* 94 (8) (2003) 4967–4971.
- [12] S.T. Huxtable, D.G. Cahill, S. Shenogin, L.P. Xue, R. Ozisik, P. Barone, M. Usrey, M.S. Strano, G. Siddons, M. Shim, P. Keblinski, Interfacial heat flow in carbon nanotube suspensions, *Nature Mater.* 2 (2003) 731–734.
- [13] Q. Huang, L. Gao, Y.Q. Liu, J. Sun, Sintering and thermal properties of multiwalled carbon nanotube–BaTiO<sub>3</sub> composites, *J. Mater. Chem.* 15 (20) (2005) 1995–2001.
- [14] R.A. Janes, M. Aldissi, R.B. Kaner, Controlling surface area of titanium nitride using metathesis reactions, *Chem. Mater.* 15 (23) (2003) 4431–4453.
- [15] Il-S. Kim, P.N. Kumta, Hydrazide sol–gel synthesis of nanostructured titanium nitride: precursor chemistry and phase evolution, *J. Mater. Chem.* 13 (8) (2003) 2028–2035.
- [16] A. Kuznetsova, I. Popova, J.T. Yates Jr., M.J. Bronikowski, C.B. Huffman, J. Liu, R.E. Smalley, H.H. Hwu, J.G. Chen, Oxygen-containing functional groups on single-wall carbon nanotubes: NEXAFS and vibrational spectroscopic studies, *J. Am. Chem. Soc.* 123 (43) (2001) 10699–10704.
- [17] G.W. Lu, B.L. Cheng, H. Shen, Y.J. Chen, T.H. Wang, Z.H. Chen, H.B. Lu, K.J. Jin, Y.L. Zhou, G.Z. Yang, Large optical third-order nonlinearity of composite thin film of carbon nanotubes and BaTiO<sub>3</sub>, *Chem. Phys. Lett.* 407 (4–6) (2005) 397–401.
- [18] G.Y. Han, J.Y. Yuan, G.Q. Shi, F. Wei, Electrodeposition of polypyrrole/multiwalled carbon nanotube composite films, *Thin Solid Films* 474 (1–2) (2005) 64–69.
- [19] J.L. Bahr, J.M. Tour, Covalent chemistry of single-walled carbon nanotubes, *J. Mater. Chem.* 12 (7) (2002) 1952–1958.
- [20] A. Gromov, S. Dittmer, J. Svensson, O.A. Nerushev, S.A. Perez-García, L. Licea-Jiménez, R. Rychwalski, E.E.B. Campbell, Covalent amino-funtionalisation of single-wall carbon nanotubes, *J. Mater. Chem.* 15 (32) (2005) 3334–3339.
- [21] L.Q. Jiang, L. Gao, Carbon nanotubes–metal nitride composites: a new class of nanocomposites with enhanced electrical properties, *J. Mater. Chem.* 15 (1) (2005) 260–266.
- [22] L.X. Benedict, S.G. Louie, M.L. Cohen, Heat capacity of carbon nanotubes, *Solid State Commun.* 100 (3) (1996) 177–180.
- [23] S. Shenogin, L. Xue, R. Ozisik, P. Keblinski, Role of thermal boundary resistance on the heat flow in carbon-nanotube composites, *J. Appl. Phys.* 95 (12) (2004) 8136–8144.
- [24] S. Shenogin, A. Bodapati, L. Xue, R. Ozisik, P. Keblinski, Effect of chemical functionalization on thermal transport of carbon nanotube composites, *Appl. Phys. Lett.* 85 (12) (2004) 2229–2231.
- [25] C.H. Liu, S.S. Fan, Effects of chemical modifications on the thermal conductivity of carbon nanotube composites, *Appl. Phys. Lett.* 86 (2005) 123106.
- [26] W. Yi, L. Lu, D.L. Zhang, Z.W. Pan, S.S. Xie, Linear specific heat of carbon nanotubes, *Phys. Rev. B* 59 (14) (1999) R9015–R9018.
- [27] C.-W. Nan, Z. Shi, Y. Lin, A simple model for thermal conductivity of carbon nanotube-based composites, *Chem. Phys. Lett.* 375 (5–6) (2003) 666–669.